A simple procedure for determination of the dynamic ship-impact load on bridge structures

W. Fan[1] & W. C. Yuan[2]
[1]*Department of Bridge Engineering, College of Civil Engineering, Hunan University, China*
[2]*State Key Laboratory of Disaster Reduction in Civil Engineering, Tongji University, China*

Abstract

An equivalent static force is usually used to represent vessel-impact load exerted on bridge structures in current bridge design codes. However, this static procedure using the code-prescribed loads cannot consider dynamic effects (e.g. inertial force related to superstructure mass). Hence, the vessel-impact responses of bridges may be significantly underestimated and the structural safety cannot be warranted in practice. In this paper, a simple procedure is proposed to define the dynamic ship-impact loads on bridge structures. Firstly, the equations to determine the duration of loading and the maximum ship-bow crush depth are developed based upon principles of conservation of energy and linear momentum during a collision event. Using the above equations and the relationships between crush depth and time, the dynamic ship-impact loads are determined based on ship bow force-deformation curves (*P-a* curves). For the generated ship-impact load histories, the amplitude, duration and frequency spectra are compared with the results from the high-resolution finite element analyses of ship-bridge collisions. It is found that these parameters are in good agreement with the high-resolution analysis results and the developed procedure can be readily employed to determine the vessel-impact responses of bridge structures like the time history analysis in seismic design.
Keywords: impact load, ship collision, bridge structure, P-a curve.

1 Introduction

The static analysis approach was firstly conducted by Minorsky [1] to assess the extent of nuclear powered ship damage during a collision. Using the data from

www.witpress.com, ISSN 1743-3509 (on-line)
doi:10.2495/SUSI140071

26 actual collisions, a semi-analytical equation was proposed to describe the relationship between the deformed steel volume and the absorbed impact energy. After this, lots of researchers focused on quantifying vessel-impact loads, e.g., Woisin [2] and Pedersen *et al.* [3]. Based on these researches, some equations were developed to determine equivalent static vessel-impact forces in current bridge design codes, e.g., AASHTO [4], BSI [5] and JTG-D60 [6] in China. However, the vessel-impact loads from various codes are significantly different, as shown in Figure 1. The reasons for these differences include that: (1) the shapes and types of vessel bows are different due to the variances of ship-building standards in different countries; (2) the code-prescribed loads are mainly developed by empirical analyses because very limited data from collision tests are available; and (3) the different characteristic values of ship-impact forces are selected as the design loads (e.g., peak force in BSI [5] and 70% fractile value in AASHTO [4]). These discrepancies also imply that further efforts should be made to reasonably define vessel impact loads. More importantly, recent experimental and analytical studies [7−9] pointed out the static analysis procedure neglects crucial dynamic amplification effects related to the mass of bridge superstructure. Thus, several alternative analysis techniques were proposed to quantify collision-induced bridge responses with dynamic amplification effects included, e.g., applied vessel impact load history method, static bracketed impact analysis (SBIA) [7] and shock spectrum analysis (SSA) [10]. All these analysis methods were based upon the use of an elastic-perfectly plastic force-deformation relationships to model barge bow stiffness [11]. However, it was found from our previous studies [12–14] that ship bow force-deformation relationships are more complicated than those of barge bow. Hence, these methods cannot be directly applied to the analyses of ship-bridge collisions.

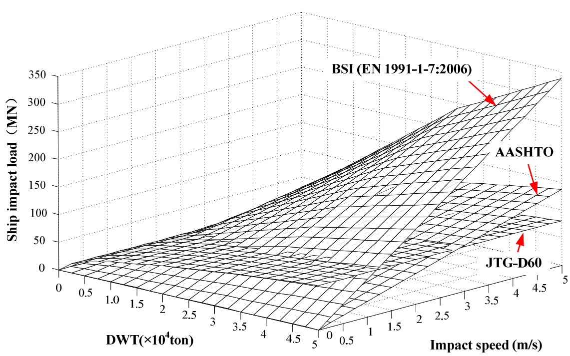

Figure 1: Comparisons of code-prescribed ship impact loads.

Based on the previous studies [12–14], a simple procedure is improved in this paper to reasonably determine the dynamic ship-impact loads of bridge structures. Firstly, ship-bridge interaction analyses are conducted using two degree-of-freedom (2-DOF) models. Equations for the peak crush depth of ship bow and duration of loading are then developed based upon principles of conservation of energy and linear momentum. The resulting equations are used to determine dynamic ship-impact loads and responses of bridge structures. Meanwhile, the amplitude, duration and frequency spectra of the generated dynamic ship-impact loads are compared with the high-resolution analysis results to validate the developed procedure.

2 Ship-bridge interaction analysis using 2-DOF model

The previous studies [12–14] indicated that the colliding ship can be modelled by a special single-degree-of-freedom (SDOF) system. Based on the ship SDOF model, a simplified interaction model with two degrees-of-freedom (DOFs) (illustrated in Fig. 1) is employed here to qualitatively address the ship-bridge interaction and provide a basis for determination of dynamic ship-impact loads. In the 2-DOF interaction model, the lumped ship mass (m_s) is connected to the mass of bridge structure (m_b) by a specific compression-only spring; m_b is linked to the ground by an assumed spring k_b.

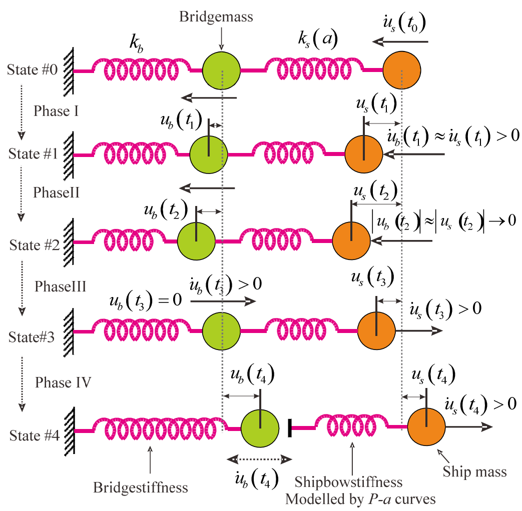

Figure 2: Interaction analysis of ship-bridge collisions using 2-DOF model.

Ideally, a ship-bridge collision consists of four interaction phases. Phase I is from initial ship-bridge contact to them with the same speeds (namely, $\dot{u}_b(t_1) \approx \dot{u}_s(t_1) > 0$, where $\dot{u}_b$ and $\dot{u}_s$ are the bridge and ship speed, respectively). At Phase II, both ship and bridge decelerate together until $|\dot{u}_b(t_2)| \approx |\dot{u}_s(t_2)| \approx 0$. Then, they accelerate in the reverse direction during Phase III. At Phase IV, the bridge mass separates from the ship SDOF system and is undergoing free vibration. In actual ship-bridge collisions, these above four phases may be not clearly identified due to the influence of the higher modes. Phase I and II can be

www.witpress.com, ISSN 1743-3509 (on-line)

regarded collectively as a loading phase, where the conservation of energy equation can be written as:

$$\underbrace{0.5\left(m_s+dm_s\right)\dot{u}_s\left(t_0\right)^2}_{KE}=\underbrace{\int_0^{a(t_2)}P\left(a\right)da}_{E_s}+\underbrace{\int_0^{u_b(t_2)}k_b u_b du_b}_{IE_b} \tag{1}$$

where $\dot{u}_s\left(t\right)$ is the ship speed at the time (t); $\dot{u}_s\left(t_0\right)$ is the initial impact speed; dm_s is the added water mass; $P(a)$ is the function of impact force with respect to ship bow crush depth (a); $u_b\left(t_2\right)$ is the bridge displacement at the end of Phase II (t_2); KE is the initial kinetic energy of ship; E_s is the internal energy of ship; IE_b is the internal energy of bridge. The conservation of linear momentum can be expressed as:

$$\int_0^{t_2}P\left(t\right)dt=\left(m_s+dm_s\right)\dot{u}_s\left(t_2\right) \tag{2}$$

where $P(t)$ is the function of impact force with respect to time (t).

3 Development of dynamic ship-impact load

3.1 Ship bow force-deformation curve

Compared with the barge [11], the ship bow force-deformation curve (denoted by *P-a* curve) is more complex due to the complicated geometry of vessel bows. To date, there are no regularized *P-a* curves that are widely accepted to represent the ship bow stiffness. Generally, the finite element crush analyses are employed to obtain the basic ship bow force-deformation curves using the numerical models in the previous studies [12–14]. Through the explicit dynamic analyses, the ship bow *P-a* curves are obtained and presented in Figure 3.

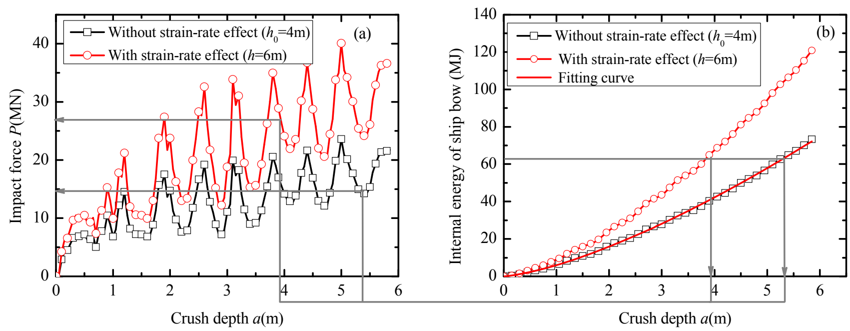

Figure 3: Ship bow *P-a* curve and the maximum crush depth estimation.

As observed in Figure 3, the strain-rate effect has a significant impact on the *P-a* curves, and should be considered to accurately define dynamic ship-impact loads on bridge structures. In addition, the depth of pile-cap contact with vessel also has a marked effect on the impact forces [12–14]. For the 5,000DWT ship, the effect of pile-cap depth can be considered by [14]:

$$\beta_h(h/H, a) = \begin{cases} 1.0, & 0 \le a < 0.95\text{m} \\ 1.23 - 0.24a \ge 0.11\exp\left(1.58\dfrac{h}{H}\right) + 0.47, & a \ge 0.95\text{m} \end{cases} \tag{3}$$

where β_h is the influence factor of pile-cap depth and the function with respect to h/H and crush depth; H is the moulded ship bow depth (H=6.4 m for 5,000DWT ship); h is the pile-cap depth. Using the basic curves in Figure 3(a) and Eq. (3), the event-specific *P-a* curves can be readily determined at different initial impact conditions.

3.2 Estimation of the maximum ship bow crush depth

As illustrated in Figure 3, the maximum crush depth ($a_{\max}$) can be readily estimated using a given E_s and the energy-deformation curve (*E-a* curve) in the left side of Figure 3. The *E-a* curves in Figure 3 are obtained from the numerical integrations of the *P-a* curves. Since The ship bow *E-a* curves are relatively regular, the numerical integration may be not necessary for each collision event, because. They can be fitted by simple functions, e.g., power, exponential and quadratic functions. For the basic energy-deformation curve (denoted by E_{sh}-a curve), the fitting parameters are tabulated in Table 1. The results from all these equations agree very well with the numerical results.

Table 1: The fitting equations of E_{sh}-a curves.

Functions		A	B	R^2
Power function	E_{sh}(a)=Aa^B	5.973×10^6	1.411	0.9995
Exponential function	$E_{sh}(a)= A\,[\exp(Ba)\text{-}1]$	3.530×10^7	0.193	0.9987
Quadratic function	$E_{sh}(a)=Aa^2+Ba$	1.152×10^6	5.803×10^6	0.9994

Note: the energy units is J and the crush depth a is m in these equations.

For a given collision event, the function of the energy-deformation curve ($E_d(a)$) can be easily determined from the functions of E_{sh}-a curve by considering the effects of strain-rate and pile-cap depth. Hence, the crush depth can be estimated by the inverse of the $E_d(a)$ function, namely

$$a(E_d) = \begin{cases} \left[E_d/(A\bar{\beta}\beta_h)\right]^{1/B} & \text{Inverse of power function (a)} \\ \dfrac{1}{B}\ln\left[E_d/(A\bar{\beta}\beta_h)+1\right] & \text{Inverse of exponential function (b)} \\ \left[-B+\sqrt{B^2+4AE_d/(\bar{\beta}\beta_h)}\right]\Big/(2A) & \text{Inverse of quadratic function (c)} \end{cases} \tag{4}$$

where A and B are the fitting parameters and given in Table 1. Several cases of ship collisions with rigid pile-caps are carried out in order to validate the rationality of Eq. (4). Comparisons of the analytical and numerical results in Table 2 show that Eq. (4) can be used to accurately estimate the maximum crush depth, particularly for the first expression in Eq. (4).

Table 2: Estimation of the maximum crush depth using Eq. (4).

$\dot{u}_s(t_0)$	Numerical	Int.	Eq.(4)			Error (%)			
			(a)	(b)	(c)	Int.	(a)	(b)	(c)
1m/s	0.512	0.551	0.524	0.340	0.385	7.67	2.41	-33.54	-24.88
2m/s	1.476	1.491	1.521	1.379	1.446	1.06	3.10	-6.52	-2.02
3m/s	2.566	2.517	2.387	2.356	2.385	-1.91	-6.98	-8.17	-7.07
4m/s	3.780	3.740	3.546	3.607	3.587	-1.07	-6.20	-4.58	-5.11
5m/s	4.972	4.951	4.818	4.851	4.831	-0.42	-3.10	-2.45	-2.83
Average error						2.43	4.36	11.05	8.38

Note: "Int." in the table means the E_d-a curve is obtained from the numerical integration of P-a curve and used to determined the crush depth.

3.3 Duration of dynamic ship-impact load

In barge-bridge collision analysis, the duration of loading can be determined only based on the elastic-perfectly plastic P-a curves and the principle of linear momentum. For the determination of ship-impact load duration, however, the relationship between crush depth (a) and time needs to be assumed beforehand. For this reason, lots of numerical analyses are conducted to obtain the deformation-time relationships, as shown in Figure 4.

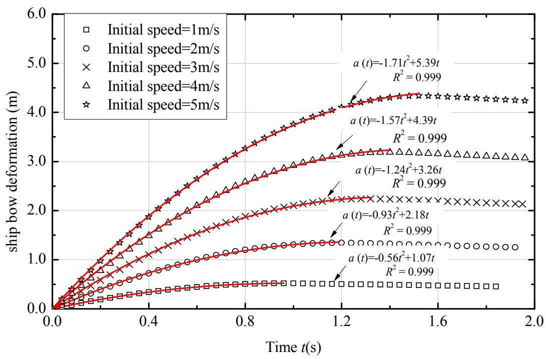

Figure 4: Time history of ship bow deformation.

It is observed from Figure 4 that these deformation curves with respect to time can be approximated by a cubic parabola before the deformation reaches the maximum value ($a_{\max}$). Thus, the a-t relationship can be assumed as:

$$a \approx \alpha_1 t^2 + \alpha_2 t \quad a \in [0, a_{\max}] \tag{5}$$

where α_1 and α_2 can be determined by the boundary conditions and expressed as

$$\begin{cases} \alpha_1 = -\dot{u}_s^2(t_0) / (4a_{\max}) \\ \alpha_2 = \dot{u}_s(t_0) \end{cases} \tag{6}$$

Using Eqs (5) to (6), the duration of the loading phase (t_{dl}) can be determined by:

$$t_{dl} = -\alpha_2 / (2\alpha_1) = 2a_{\max} / \alpha_2 = 2a_{\max} / \dot{u}_s(t_0) \tag{7}$$

However, it should be noted that the fitting equations in Figure 4 are different from Eq. (5) with the coefficients in Eq. (6). During a collision event, t_{dl} obtained from Eq. (7) differs from the actual duration during a collision event. As a result, the principle of linear momentum cannot be satisfied for ship-bridge collision system. Therefore, the correction for t_{dl} should be made to meet the principle of linear momentum. It is assumed that the value estimated by Eq. (7) is called as ${}^0t_{dl}$ and the actual value is ${}^1t_{dl}$. Using Eq. (2), the impulse ratio for two different t_{dl} can be written as:

$$\frac{\int_0^{{}^0t_{dl}} P_d(t)\,dt}{\int_0^{{}^1t_{dl}} P_d(t)\,dt} = \frac{\int_0^{{}^0t_{dl}} P_d(t)\,dt}{(m_s + dm_s)\dot{u}_s(t_0)} = \frac{\int_0^{{}^0t_{dl}} P_d(t)\,dt \Big/ (m_s + dm_s)}{\dot{u}_s(t_0)} \tag{8}$$

Based on the mean value theorem for integrals, the impulse ratio can be re-written as:

$$\int_0^{{}^0t_{dl}} P_d(t)\,dt \Big/ \int_0^{{}^1t_{dl}} P_d(t)\,dt = P_d(\xi_1)\,{}^0t_{dl} \Big/ \left[P_d(\xi_2)\,{}^1t_{dl}\right] \tag{9}$$

where $\xi_1 \in [0, {}^0t_{dl}]$; $\xi_2 \in [0, {}^1t_{dl}]$. Substituting Eq. (7) into Eq. (9),

$$\int_0^{{}^0t_{dl}} P_d(t)\,dt \Big/ \int_0^{{}^1t_{dl}} P_d(t)\,dt = P_d(\xi_1)\alpha_2 \Big/ \left[P_d(\xi_2)\dot{u}_s(t_0)\right] \tag{10}$$

Assuming $P_d(\xi_1) \approx P_d(\xi_2)$ and comparing Eq. (10) with Eq. (8), the nominal impact speed (α_{2n}) can be expressed as

$$\alpha_{2n} = \int_0^{{}^0t_{dl}} P_d(t)\,dt \Big/ (m_s + dm_s) \tag{11}$$

Therefore, ${}^1t_{dl}$ can be written as

$${}^1t_{dl} = 2a_{\max} / \alpha_{2n} = 2a_{\max}(m_s + dm_s) \Big/ \int_0^{{}^0t_{dl}} P_d(t)\,dt \tag{12}$$

Similarly, the collision cases in Table 2 are employed to validate Eq. (12) and the corresponding results are presented in Table 3.

For the unloading phase, the duration can be determined from the method proposed by Cowan [9]. Thus, the unloading duration (t_{du}) can be obtained by

$$t_{du}=0.5\pi\sqrt{\left(m_s+dm_s\right)/K_u} \tag{13}$$

where $K_u=(1/k_{su}+1/k_{bu})^{-1}$, where k_{su} and k_{bu} is the unloading stiffness for ship and bridge, respectively. For 5,000DWT ship, the unloading stiffness is 1.55×10^9N/m, which were determined by a number of numerical analyses in [14].

Table 3: Duration estimation for the loading phase.

$\dot{u}_s(t_0)$	t_{dl}			Error (%)	
	Numerical	${}^0t_{dl}$	${}^1t_{dl}$	${}^0t_{dl}$	${}^1t_{dl}$
1m/s	0.94	1.10	0.96	17.28	2.04
2m/s	1.46	1.49	1.40	2.14	-4.05
3m/s	1.49	1.68	1.37	12.62	-8.38
4m/s	1.63	1.87	1.61	14.71	-1.31
5m/s	1.70	1.98	1.66	16.50	-2.51
Average error				12.65	3.66

3.4 Determination of dynamic ship-impact load

Based on the above discussions, the procedure for determination of ship-impact load is summarized by the flow chart presented in Figure 5.

This procedure mainly consists of two sub-procedures. The first sub-procedure aims at reasonably estimating the maximum crush depth ($a_{\max}$). The second sub-procedure is used to determine the ship-impact load history. In the previous studies [15], the internal energy (IE_b) of the collided bridges was assumed to be zero during the determination of the vessel-impact load. However, Cowan [9] pointed out that it was very important to account for the influence of IE_b on ship-impact load history. As illustrated in Figure 5, a simple iterative sub-procedure is employed to consider the influence of IE_b and accurately determine E_s for the estimation of $a_{\max}$. Then, the duration of the ship-impact force history is determined by Eqs (7), (12) and (13). Using the assumed relationships between crush depth and time, the ship-impact load history is developed by means of the *P-a* curves and the above parameters. Finally, the dynamic analysis of ship-bridge collision can be determined using the developed ship-impact load history, like the time history analysis in the seismic design of bridge.

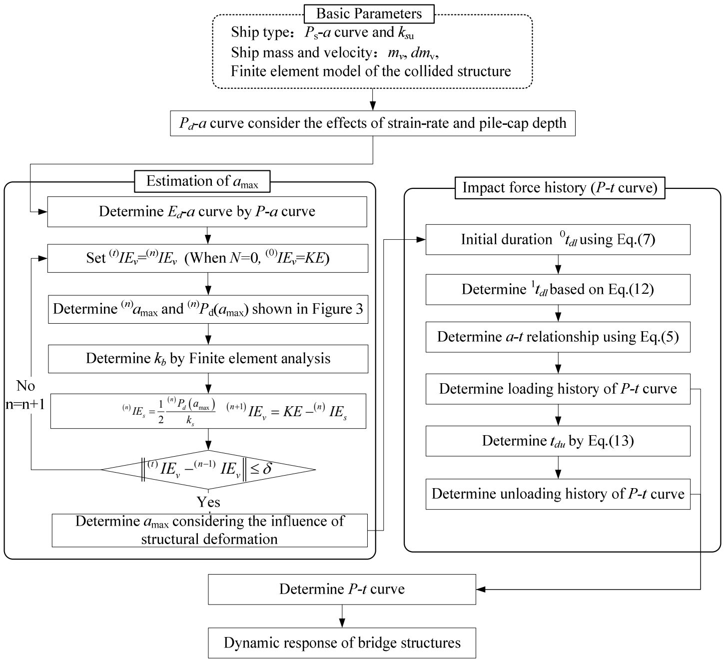

Figure 5: Flow chart of the determination of dynamic ship-impact load.

4 Application and discussions

The 5000DWT ship collisions with a six-span continuous girder bridge are selected to discuss the rationality of the proposed procedure for determining ship-impact loads. The high-resolution finite element model is generated as illustrated in Figure 6. The time history analysis model shown in Figure 7 is employed to conduct the dynamic analysis of ship-bridge collision. In the time history analysis model, the dynamic ship-impact load is employed to represent the action of ship collision. Apparently, the computational efficiency of the time history analysis model will be improved greatly compared with the contact-impact simulation of ship-bridge collisions in Figure 6.

Two different initial impact speeds of 2 m/s and 4 m/s are investigated respectively. The former one is the maximum current speed at the bridge site, while the latter one is the design impact speed determined by the channel arrangement, typical vessel transit speed and overall length of the ship [4].

As shown in Figure 8, the ship-impact force histories obtained from the proposed procedure are in good agreement with the results from high-resolution finite element analyses. In addition, the wavelet spectra of ship-impact force histories are calculated to compare their frequency characteristics. Similarly, their wavelet spectra are very similar to each other. Furthermore, comparisons of

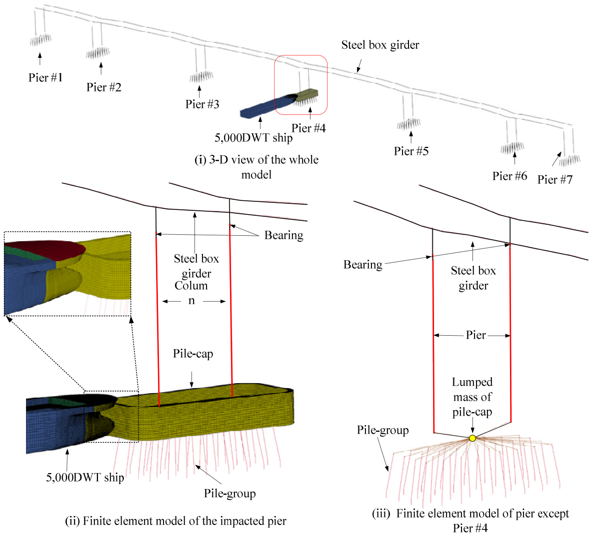

Figure 6: High-resolution finite element model of ship-bridge collision.

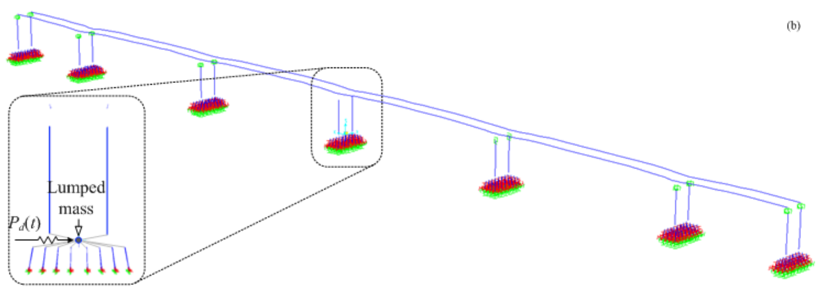

Figure 7: Time history analysis model of ship-bridge collision.

the dynamic responses from two different models are carried out and presented in Figure 10. It can be found that their peak responses are very close and their Pearson's correlations are very clear (all Pearson's *r* are close to 1.0). Therefore, all these results imply that the ship-impact load histories are reasonable and the proposed procedure can be available in the ship-bridge collision analysis. Undoubtedly, the computational efficiency using the proposed procedure is significantly improved in comparison with the high resolution finite element analysis. In addition, since the time history of ship-impact loads replace the complicated contact definition in the high-resolution finite element model, several difficult issues (i.e., hourglass control and numerical stability) are avoided together.

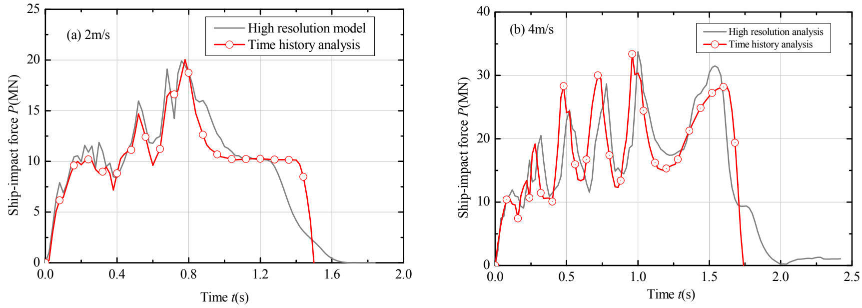

Figure 8: Time history of ship-impact force (a) initial impact speed of 2m/s; (b) initial impact speed of 4m/s.

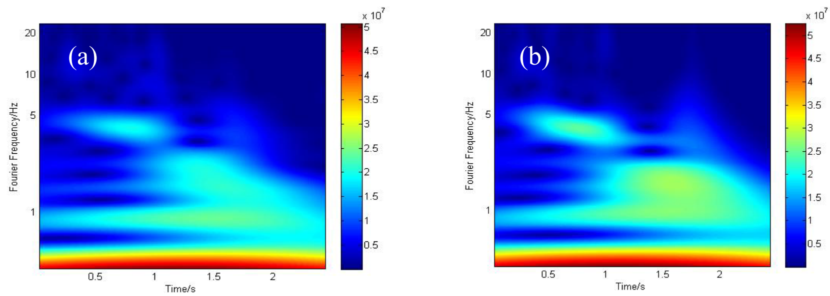

Figure 9: Comparison of wavelet spectrum at the impact speed of 4 m/s.

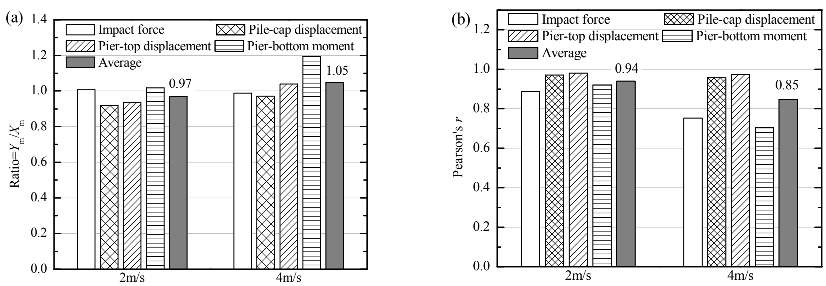

Figure 10: Correlation analysis (a) comparison of peak responses; (b) Pearson's correlation analysis.

5 Conclusions

A simple procedure was proposed in this paper to determine dynamic ship-impact loads and conduct the time history analysis of ship-bridge collision. The following conclusions can be drawn:

(1) The maximum ship bow crush depth can be determined based upon the principle of energy conservation. The equations to estimate the maximum crush depth were developed and validated.

(2) The equations was developed to determine ship-impact load duration and validated for several collision events. It was found that the correction for the initial duration estimation should be made to approximate the expected results.

(3) The flow chart of the determination of dynamic ship-impact load were summarized and applied into the 5,000DWT ship collisions with a continuous girder bridge. It was observed from the case studies that the amplitude, duration and wavelet spectra of the ship-impact loads and the resulting responses were in good agreement with the results of high-resolution finite element analysis.

Acknowledgements

This research is supported by the National Science Foundation of China (Grant No. 51308202 and 51278376), Research Fund for the Doctoral Program of Higher Education of China (Grant No. 20130161120026) and Hunan Provincial Natural Science Foundation of China (Grant No. 14JJ3056).

References

[1] Minorsky, V.U. An Analysis of Ship Collision to Protection of Nuclear Power Plant. *Journal of Ship Research* 1, pp. 1-4, 1959.

[2] Woisin, G. The Collision Tests of the GKSS. Jahrbuch der Schiffbautechnischen Gesellschft, Berlin, Germany; 1976. p. 465-87.

[3] Pedersen, P.T., Valsgaard, S., Olsen, D., Spangenberg, S. Ship impacts: bow collisions. *Int J Impact Eng* 13, pp. 163-87, 1993.

[4] AASHTO. Guide Specifications and Commentary for Vessel Collision Design of Highway Bridges. 2nd edition ed. Washington, D.C.: American Association of State Highway and Transportation Officials; 2009.

[5] BSI. Eurocode 1: Actions on Structures—Part 1-7: General Actions-Accidental Actions. Part 1-7: General Actions-Accidental Actions. London, UK, 2006.

[6] Ministry of Communications. General Code for Design of Highway Bridges and Culverts (JTG D60-2004). Beijing: China Communications Press; 2004.

[7] Getter, D.J., Consolazio, G.R., Davidson, M.T. Equivalent Static Analysis Method for Barge Impact-Resistant Bridge Design. *J Bridge Eng* 16, pp. 718-27, 2011.

[8] Consolazio, G.R., Cowan, D.R. Numerically efficient dynamic analysis of barge collisions with bridge piers. *J Struct Eng-ASCE* 131, pp. 1256-66, 2005.

[9] Cowan, D.R. Development of time-history and response spectrum analysis procedures for determining bridge response to barge impact loading [PhD. Dissertation]. FL.: University of Florida; 2007.

[10] Fan, W., Yuan, W.C. Shock spectrum analysis method for dynamic demand of bridge structures subjected to barge collisions. *Comput Struct* 90-91, pp. 1-12, 2012.

[11] Consolazio, G.R., Davidson, M.T., Cowan, D.R. Barge Bow Force-Deformation Relationships for Barge-Bridge Collision Analysis. *Transportation Research Record*, pp. 3-14, 2009.
[12] Fan, W., Yuan, W.C., Yang, Z., Fan, Q.W. Dynamic Demand of Bridge Structure Subjected to Vessel Impact Using Simplified Interaction Model. *J Bridge Eng* 16, pp. 117-26, 2011.
[13] Fan, W., Yuan, W., Yang, Z., Fan, Q. Development of time history analysis for dynamic demand of elevated pile-cap bridge subjected to vessel collision. *Journal of Tongji University Natural Science* 38, pp. 1719-24, 2010.
[14] Fan, W. Dynamic demand of bridge structures and capacity of pile-supported protection structures under vessel impacts. Shanghai: PhD dissertation, Tongji University, Shanghai, China; 2012.
[15] IABSE. IABSE Colloquium on Ship Collision with Bridges and Offshore Structures, 3Vol. (Introductory, Preliminary, and Final Reports). Copenhagen, Denmark: International Association of Bridge and Structural Engineers; 1983.